

Mineralization
How to cite: *Angew. Chem. Int. Ed.* **2021**, *60*, 16707–16713

International Edition: doi.org/10.1002/anie.202104002

German Edition: doi.org/10.1002/ange.202104002

Uncovering the Role of Bicarbonate in Calcium Carbonate Formation at Near-Neutral pH

Yu-Chieh Huang, Ashit Rao, Shing-Jong Huang, Chun-Yu Chang, Markus Drechsler, Jennifer Knaus, Jerry Chun Chung Chan, Paolo Raiteri, Julian D. Gale, and Denis Gebauer*

Abstract: Mechanistic pathways relevant to mineralization are not well-understood fundamentally, let alone in the context of their biological and geological environments. Through quantitative analysis of ion association at near-neutral pH, we identify the involvement of HCO_3^- ions in CaCO_3 nucleation. Incorporation of HCO_3^- ions into the structure of amorphous intermediates is corroborated by solid-state nuclear magnetic resonance spectroscopy, complemented by quantum mechanical calculations and molecular dynamics simulations. We identify the roles of HCO_3^- ions as being through (i) competition for ion association during the formation of ion pairs and ion clusters prior to nucleation and (ii) incorporation as a significant structural component of amorphous mineral particles. The roles of HCO_3^- ions as active soluble species and structural constituents in CaCO_3 formation are of fundamental importance and provide a basis for a better understanding of physiological and geological mineralization.

Introduction

Reactions of nucleation and crystallization operating at distinct spatiotemporal scales make critical contributions to biological and geological phenomena, where calcium carbonate (CaCO_3) is an important scientific model system for investigating the molecular mechanisms of these processes. The quest for an understanding of CaCO_3 formation is particularly intense due to the ecological, geological, and industrial relevance of this system.^[1] Although extensive studies have been dedicated to the nucleation and crystallization of CaCO_3 , the underlying mechanisms of mineral

formation and growth are still under debate. Classical nucleation theory provides a fundamental framework for understanding the onset of phase separation, that is, nucleation.^[2,3] However, the existence of solute ion clusters in undersaturated and supersaturated solutions,^[4] polymer-induced liquid precursors,^[5,6] and amorphous intermediates^[7–10] as precursors of several biological and synthetic materials has provided a new perspective on the classical notions of nucleation and crystallization.^[8,11–13]

While numerous works have shown that classical nucleation theory (CNT) is, in principle, useful for evaluating and describing the nucleation of calcium carbonate,^[14,15] alternative notions of nucleation involving stable pre-nucleation clusters (PNCs) have been developed.^[4] Regarded as thermodynamically stable solute entities, PNCs exist in equilibrium with the free ions and ion pairs prior to nucleation.^[4,16,17] It has to be noted that some interpretations of cryo-TEM images were recently revoked,^[18] however, and the existence of PNCs was fundamentally challenged.^[18,19] This criticism has been rejoined elsewhere,^[3] showing the notions of the PNC pathway remain a sound basis for interpretation of experimental data. Indeed, very recently, a quantitative model for the experimentally verified liquid–liquid miscibility gap in the aqueous calcium carbonate system has been introduced, demonstrating the predictive power of the PNC model.^[20] Specifically, the model predicts the loci of the binodal and spinodal curves accounting for amorphous polymorphism, and the critical point of the liquid–liquid phase diagram, based on the original PNC model that assumes equal and independent ion association in each step

[*] Prof. Dr. D. Gebauer
 Institute of Inorganic Chemistry
 Leibniz University of Hannover
 Callinstr. 9, 30167 Hannover (Germany)
 E-mail: gebauer@acc.uni-hannover.de

Dr. Y.-C. Huang, Dr. J. Knaus
 Department of Chemistry, Physical Chemistry
 University of Konstanz, Konstanz (Germany)


Dr. A. Rao
 Physics of Complex Fluids Group and MESA+ Institute
 Faculty of Science and Technology
 University of Twente, Enschede (The Netherlands)


Dr. S.-J. Huang, C.-Y. Chang, Prof. Dr. J. C. C. Chan
 Department of Chemistry, National Taiwan University
 Taipei 106 (Taiwan)

Dr. M. Drechsler
 Bavarian Polymer Institute
 University of Bayreuth (Germany)

Dr. J. Knaus
 stimOS GmbH
 Konstanz (Germany)

Assoc. Prof. Dr. P. Raiteri, Prof. Dr. J. D. Gale
 Curtin Institute for Computation/
 The Institute for Geoscience Research (TiGer)
 School of Molecular and Life Sciences
 Curtin University, Perth (Australia)

 Supporting information and the ORCID identification number(s) for the author(s) of this article can be found under:
<https://doi.org/10.1002/anie.202104002>.

 © 2021 The Authors. *Angewandte Chemie International Edition* published by Wiley-VCH GmbH. This is an open access article under the terms of the Creative Commons Attribution Non-Commercial License, which permits use, distribution and reproduction in any medium, provided the original work is properly cited and is not used for commercial purposes.

toward the formation of PNCs. While the latter major assumption underlying the PNC theory remains difficult to prove or disprove unambiguously,^[21] the successful quantitative prediction of the phase behavior strongly suggests that it is indeed sustainable.^[20] The PNC pathway considers the precipitation of mineral particles from dilute solutions as a complex and multistep sequence of processes, based on the initial clustering of ions accompanied by the release of hydration water,^[22] the formation of transient liquid condensed phases via liquid–liquid demixing,^[23,24] the aggregation of the nanodroplets that are formed due to the decrease in interfacial surface area, and the subsequent precipitation of hydrated amorphous calcium carbonate (ACC) particles due to solidification of the liquid precursors.

With these developments in the field of calcium carbonate nucleation and crystallization, it has to be realized that the pH regime below ca. pH 8.5–9.0 has not been explored quantitatively, owing to technical difficulties that arise from the strong and increasing outgassing of CO₂—even though the mechanistic effects of near-neutral pH levels are of ultimate relevance in biological and geological environments. Given that the pH of seawater is between 7.5 and 8.4, the understanding of mineral nucleation in this pH regime is vital for gaining fundamental insights into physiologically relevant biomineralization mechanisms and also for assessing the crucial impacts of environmental factors such as pollution and climate change on aquatic life.^[25] Computer simulations identify distinct configurations of PNCs, with HCO₃⁻ ions occupying the ends of the molecular motifs serving as chain terminators.^[26] For instance, at pH 8.5, an excess of HCO₃⁻ ions limits the cluster chain length relative to that at high pH.^[26] Transiently formed in the course of mineral nucleation, liquid-like states of calcium carbonate are suggested to be relatively stable especially at close to neutral pH,^[27] due to a kinetic stabilization effect of HCO₃⁻ ions.^[28]

In this study, the pathways of mineral nucleation for calcium carbonate are investigated under constant near-neutral pH conditions by adapting and using quantitative potentiometric titration as the basic methodology, resolving the previously limiting issues of CO₂ in- and out-gassing. In the pH regime below pH 9.0, the relative fraction of bicarbonate in the buffer equilibrium is dominant, while the carbonate fraction decreases and becomes minor already at pH 8.5, and the fraction of CO₂ continually increases with further decreasing pH. Thus, the strategy of lowering the pH step by step starting at pH 9.0, while exploring the early stages of calcium carbonate precipitation at constant pH levels, allows the assessment of the effects of a strongly increased bicarbonate concentration relative to carbonate at near-neutral basic pH conditions, at which calcium carbonate formation is still possible. Lowering the pH further, the progressive shift of the equilibrium toward CO₂ in the near-neutral acidic regime eventually prevents mineralization. Compositional and structural insights into intermediate forms and mineralization products forming under these conditions are provided by cryogenic transmission electron microscopy (cryo-TEM), Fourier transform infrared (FTIR) spectroscopy, thermogravimetric analysis, solid-state nuclear magnetic resonance (ssNMR) spectroscopy, simulations, and quantum

mechanical calculations. Collectively, we identify previously unknown, distinct mechanistic contributions of bicarbonate ions as (i) soluble ion species with a competitive role in the ion association tendencies in regimes prior to nucleation and also (ii) an integral structural component of emergent amorphous calcium carbonates at near-neutral pH values.

Results and Discussion

As discussed in detail in the SI, Results and Discussion sections 1.1–1.3, the out-diffusion of CO₂ from bicarbonate buffers in the near-neutral pH regime can be quantitatively taken into account by means of counter-titration with dilute HCl solution (SI Figures S1–S6, Table S1). This, in turn, allows the fully quantitative assessment of pre-nucleation ion association down to pH ≈ 8.0 upon slow dosing of calcium solutions into bicarbonate buffers. In this pH regime, the fraction of bicarbonate ions becomes larger than 97% below pH 8.5, while the fraction of carbonate becomes minor, and decreases considerably further with decreasing pH (SI Table S1). Still, calcium carbonate ion association can be observed and assessed in this pH regime and is in accord with the literature (SI Table S2). However, at, and below, pH 8.5 calcium bicarbonate association must be taken into account, which is ca. two orders of magnitude weaker than calcium carbonate association, based on the respective equilibrium constants (SI Table S2). These correspond to standard Gibbs free energies of –18.43 and –7.42 kJ mol⁻¹ for the formation of CaCO₃⁰ and CaHCO₃⁺, respectively, showing that although the calcium bicarbonate interaction is considerably weaker than for calcium carbonate, it can still play a critical role during mineral pre-nucleation stages at near-neutral pH values (Figure 1, SI Results and Discussion sections 1.1–1.3, Figures S7–S9, and section 2.1).

The thermodynamics of CaCO₃ ion association into clusters prior to mineral nucleation at pH 8.0, 8.2, and 8.5 can be evaluated using a multiple binding model (SI Results and Discussion section 1.4 and 2.1). The model assumes that in a microscopic picture, the CO₃²⁻ ions have more than just one binding site for Ca²⁺ ions, as required for cluster formation. As opposed to pH 9.0–10.0, where the binding strength in cluster entities varies and provides a link between the pre- and post-nucleation speciation (more stable clusters yield more stable amorphous calcium carbonate, and vice versa),^[4,20] below pH 8.5, there are no significant changes (SI Table S3).

For the association between Ca²⁺ and HCO₃⁻ ions, on the other hand, the model yields unphysical, negative values (SI Table S4). This suggests that calcium bicarbonate association does not proceed significantly beyond ion pairing, owing to the very weak interaction free energy, as opposed to calcium carbonate. This inference has been confirmed by computer simulations from which the equilibrium constants for the association of multiple bicarbonate species with calcium ions were determined (SI Results and Discussion section 2.2). Successive standard free energies of –7.8, –2.9, and +3.3 kJ mol⁻¹ were obtained for addition of bicarbonate to Ca²⁺_(aq) to form Ca(HCO₃)_x^{2-x}, for x = 1, 2 and 3, respectively,

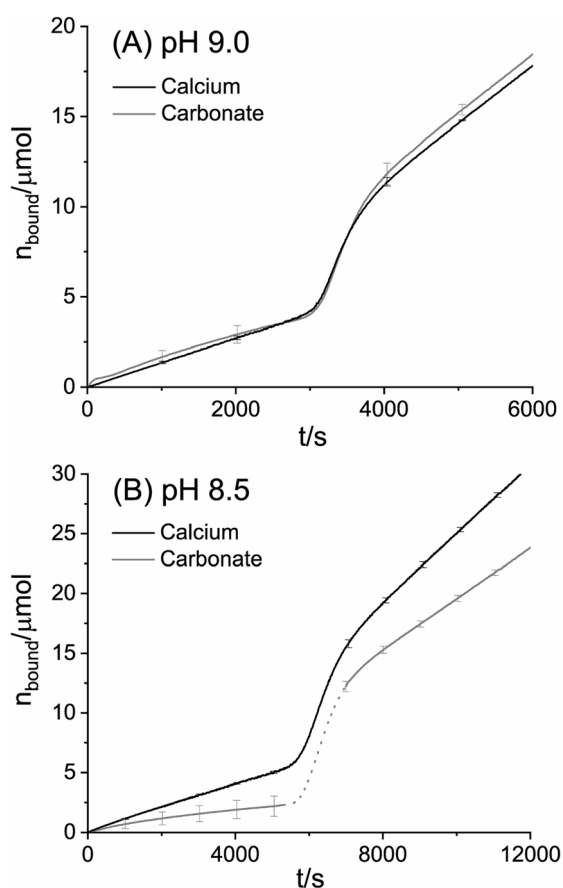


Figure 1. Time development of bound Ca^{2+} and bound CO_3^{2-} (black lines and gray lines) at A) pH 9.0 and B) pH 8.5 (CaCl_2 (10 mM) titrated into carbonate buffer (10 mM) at a constant rate). The deviation between the curves at pH 8.5 (B) is due to calcium bicarbonate association, which is negligible at pH 9.0 (A). Error bars represent $\pm 1-\sigma$ -standard deviation ($N=3$). Data at lower pH levels are shown in SI Figure S7. Detailed discussion and data evaluation can be found in SI Results and Discussion sections 1.1–1.3 and 2.1.

indicating that the corresponding species beyond ion pairing would not form appreciably at experimental conditions (SI Figure S10, S11, Table S5, S6). Using the ion association constants, it is also possible to predict the $\text{p}K_a$ shift experienced by bicarbonate as a function of coordination number by calcium. The $\text{p}K_a$ values of $\text{Ca}(\text{HCO}_3)^+$ and $\text{Ca}_2(\text{HCO}_3)^{3+}$ are estimated to be 8.6 and 6.6, respectively, as compared to 10.3 for free bicarbonate in aqueous solution (see Table 1, Figure S12 and Table S7). These values further support the assertion that bicarbonate can only bind to a single calcium under the pH conditions being considered since a bridging anion would deprotonate to give carbonate.

Table 1: Proton acidity estimated from the cluster formation free energies computed in this work and simple thermodynamic cycles similar to the one shown in Figure S12.

	$\text{p}K_a$
HCO_3^-	10.3 (experimental)
CaHCO_3^+	8.6
$\text{CaHCO}_3\text{Ca}^{3+}$	6.6

However, due to the non-equivalent association between Ca^{2+} and CO_3^{2-} ions (Figure 1, Figure S7), and the potential binding of bicarbonate ions to calcium carbonate PNCs as terminal groups, the involvement of bicarbonate in calcium carbonate nucleation certainly cannot be excluded at this point. According to the PNC pathway,^[29] calcium carbonate PNCs serve as direct molecular precursors to the phase-separated liquid nanodroplets. Indeed, nucleation occurs at constant levels of bound calcium carbonate, whereas the bound calcium bicarbonate does not seem to play a role (Figure S13). It must be noted that this very observation has been previously used to underscore the applicability of CNT,^[18] but as subsequently shown elsewhere, this argument is not necessarily sustainable.^[3] As calcium bicarbonate association does not proceed beyond ion pairs, it can thus participate in phase separation when bound to terminal binding sites of carbonate PNCs or at the interface of the nascent calcium carbonate nanodroplets, as suggested by previous simulation work.^[26] Since no solid bicarbonate-containing calcium carbonate phases have been known to occur at ambient conditions in aqueous pathways, to the best of our knowledge, bicarbonate incorporation based on CNT-type pre-/critical nuclei could only occur due to random processes, and/or at later stages of particle growth, for instance, serving as charge balance, or via surface entrapment.

Samples taken from the titration experiments at times close to nucleation were investigated by cryo-TEM (Figure 2) and show structures with diameters of 100–200 nm and low electron density contrast without clear interphase boundaries. These characteristics are evidence for hydrated, liquid-like mineral intermediates, suggestive of liquid condensed phases similar to recent experiments at higher pH.^[19] At low pH as investigated here, these liquid-like precursors are considerably more abundant and present throughout the vitrified samples (Figure S14). This apparent kinetic stabilization of the liquid intermediates at near-neutral pH may be based on the inclusion of interface-bound bicarbonate upon aggregation of nanodroplets, which may inhibit their dehydration^[27] and also introduce colloidal stabilization due to charges at the nanodroplets' surfaces, similar to effects observed in the presence of silica.^[17] This implies that bicarbonate ions become incorporated in the solid ACCs upon dehydration of the liquid precursors. Indeed, at pH 8.5, the solubility product of the initially formed phase agrees with that of proto-calcite ACC, which is approximately $3.0 \times 10^{-8} \text{ M}^2$.^[4,30] However, the solubility products of initially precipitated phases at pH 8.2 and 8.0, where the role of bicarbonate becomes significant, correspond to $3.7 \times 10^{-8} \text{ M}^2$ and $3.8 \times 10^{-8} \text{ M}^2$, respectively (Figure 3, S15). These higher values might either correspond to distinct proto-structured forms of amorphous calcium carbonate,^[30] or indicate that bicarbonate ions can enhance the solvation through a thermodynamic destabilization of the ACC when incorporated into the structure. Therefore, these metastable amorphous phases were characterized with respect to their compositional and structural nature.

Amorphous CaCO_3 (ACC) was isolated from the titration assay by a quench in excess ethanol via quick drying of the liquid–liquid phase-separated pre-nucleation state. That is,

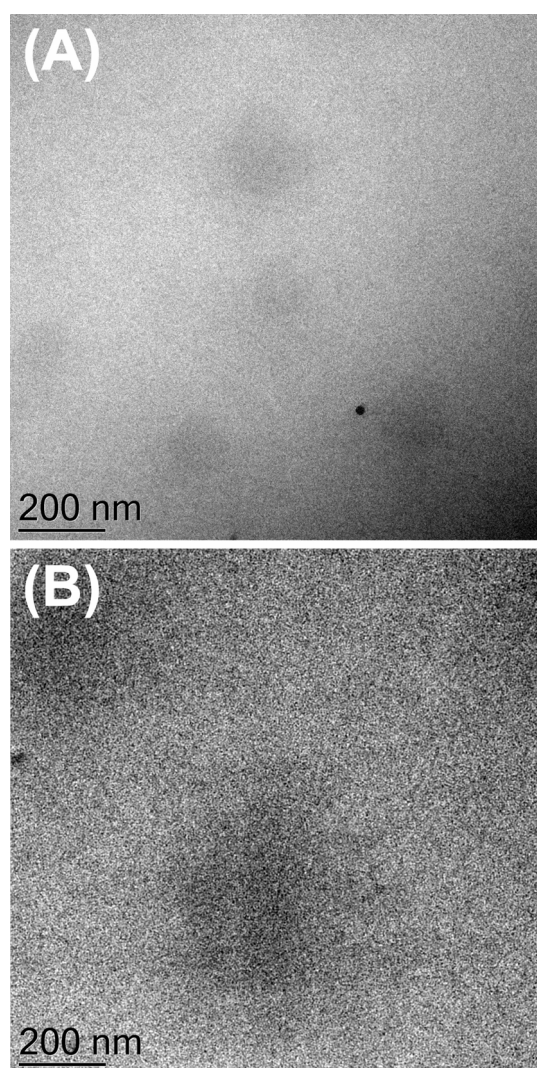


Figure 2. Representative cryo-TEM images of liquid-like phases at the pre-nucleation stages of titration experiments conducted at A) pH 8.5, B) pH 8.0.

ACCs were obtained from equilibrated, though metastable, liquid-liquid-separated states. To address the effects of near-neutral pH conditions on the composition and structure of the as-isolated amorphous mineral phases, ^{13}C -enriched (99.9%) specimens were characterized utilizing ssNMR techniques, which were complemented by quantum mechanical calculations to determine the chemical shifts for a range of environments within ACC (Tables S8–S10). As opposed to proto-calcite and proto-vaterite ACC, the $^{13}\text{C}\{^1\text{H}\}$ CPMAS spectra of samples prepared at pH 8.5, 8.0, and 7.5 do not display single Gaussian environments and were deconvoluted into two spectral components (Figure 4).

The chemical shift of the major component at the given pH is 168.8 ppm with a line width of 3.7 ppm (Figure 4, S16), both of which are in line with the values for proto-calcite ACC within experimental accuracy,^[30] and also consistent with the computed range of shifts of 163.9–171.3 ppm (average 167.9 ppm) for our model ACC with the same composition (SI section 2.4). This interpretation is further supported by

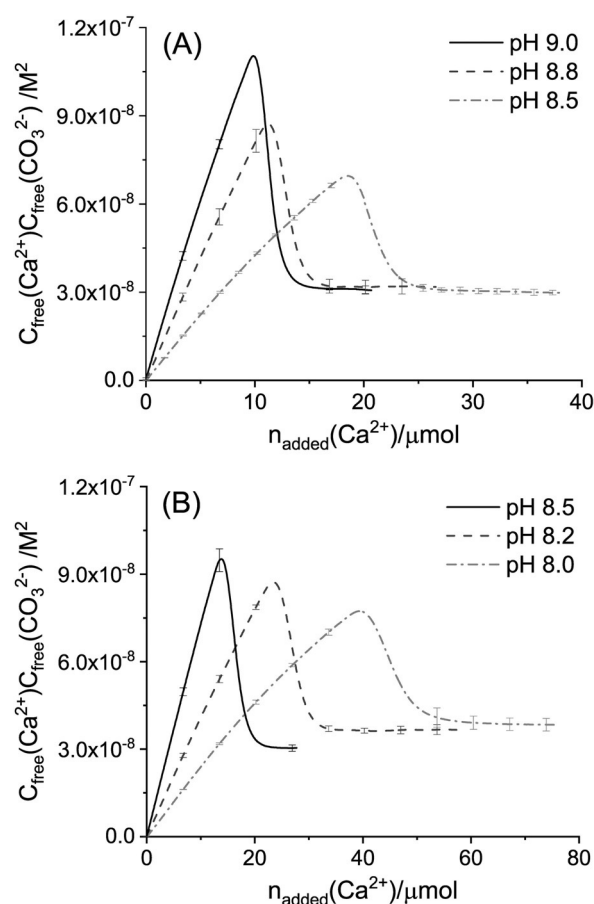


Figure 3. Development of ion products for titrations conducted at A) pH 9.0, 8.8, and 8.5 (CaCl_2 (10 mM) and carbonate buffer (10 mM)) and B) pH 8.5, 8.2, and 8.0 (CaCl_2 (20 mM) and carbonate buffer (20 mM)). The lines represent the average of three measurements, while the error bars denote $\pm 1-\sigma$ -standard deviation.

the IR spectral characteristics with bands at 1074 cm^{-1} (ν_1), 862 cm^{-1} (ν_2), and 692 cm^{-1} (ν_4) for amorphous samples synthesized at pH 7.5, 8.0, and 8.5, in accord with that of proto-calcite ACC prepared at pH 9.0^[30] (Figure S17). Since the proto-structure of the ACC remains proto-calcite below pH 9.0 (Figure 4, S16, S17), the higher solubility threshold (Figure 3) supports the role of bicarbonate ions as a structural component of ACC. Indeed, the minor component in the $^{13}\text{C}\{^1\text{H}\}$ CPMAS spectra at 163.0 ppm with a line width of 6.4 ppm corresponds to the ^{13}C chemical shift of bicarbonate species^[31,32] (Figure 4).

In order to elucidate the respective contents of carbonate and bicarbonate species in the amorphous mineral produced at distinct pH values, ^{13}C MAS spectra obtained by direct excitation of carbon via a single 90° pulse were deconvoluted based on the parameters acquired from $^{13}\text{C}\{^1\text{H}\}$ CPMAS spectra, where the optimal fit was achieved by varying the intensities (Table 2, Figure S18). The content of carbonate species shows no significant pH-dependence and approximately 5% of bicarbonate is detected in the ACC samples (Table 2). To further elucidate the spatial arrangement of carbonate and bicarbonate species, 2D $^{13}\text{C}\{^1\text{H}\}$ heteronuclear correlation (HETCOR) experiments were performed for

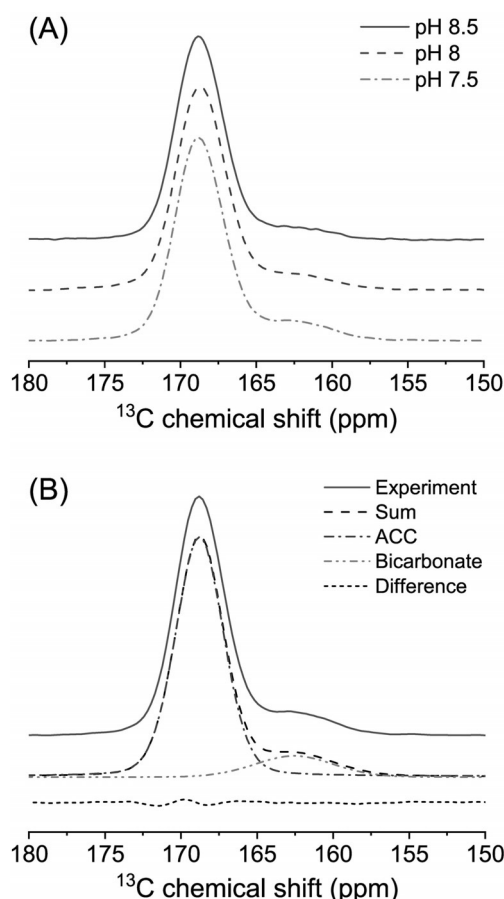


Figure 4. A) $^{13}\text{C}\{^1\text{H}\}$ CPMAS spectra of ACCs synthesized at distinct pH values as indicated. B) Spectral deconvolution for a specimen prepared at pH 7.5 (gray line), where the chemical shifts at 168.8 ppm and 162.6 ppm with line widths of 3.7 ppm and 6.1 ppm correspond to chemical shifts of proto-calcite ACC (dashed dotted dark gray line) and bicarbonate (dashed double dotted gray line), respectively. The sum of the spectral components is represented as the dashed black line, while the difference between the sum and the experiment is the short-dashed black line at the bottom.

Table 2: NMR parameters (chemical shift δ_{iso} and full width at half maximum $\Delta\nu_{1/2}$) of spectral components deconvoluted from ^{13}C MAS spectra and their relative content in the ACCs at particular pH values.

pH	Component	δ_{iso} [ppm]	$\Delta\nu_{1/2}$ [ppm]	Relative content [%]
8.5	pc-ACC	168.8	3.7	94.4
	bicarbonate-ACC	163.5	7.3	5.6
8.0	pc-ACC	168.7	3.8	94.9
	bicarbonate-ACC	162.8	6.6	5.1
7.5	pc-ACC	168.8	3.8	95.2
	bicarbonate-ACC	162.6	6.3	4.8

a sample prepared at pH 7.5 (Figure 5), while calculations were used to study a range of bicarbonate incorporation mechanisms in ACC at concentrations in the range of 2.7–5.4% (Table S10). The correlation peak in the ^1H and ^{13}C dimensions at 12.4 ppm and 161.8 ppm, respectively, provides strong evidence for the existence of bicarbonate

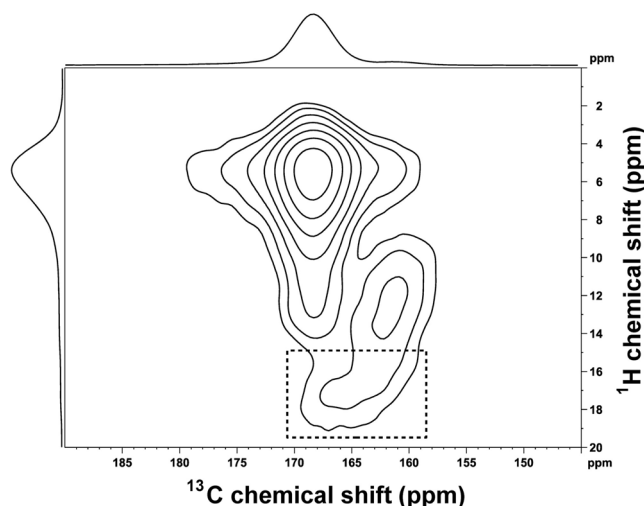


Figure 5. $^{13}\text{C}\{^1\text{H}\}$ FSLG-HETCOR spectrum acquired for ACC synthesized at pH 7.5. The spectral component at 5.5 ppm (^1H) and 168.8 ppm (^{13}C) corresponds to the correlation peak between structural water and the carbonate ions of ACC, whereas the one at 12.4 ppm and 161.8 ppm represents the $^1\text{H}/^{13}\text{C}$ correlation within the bicarbonate ions. The correlation peak at 17.2 ppm and 166.2 ppm highlighted by the dashed squared area is assigned to a species in ACC where a proton is shared almost equally between two carbonate anions.

species as a structural unit of the amorphous mineral. This closely matches the most stable site identified theoretically for a bicarbonate substitution for carbonate, where the corresponding chemical shifts are 12.1 and 162.4 ppm, respectively (Table S10). Structurally this site is found to be a bicarbonate with a hydrogen bond distance of 1.612 Å to CO_3^{2-} at the interfacial region between a dry ACC region and several water molecules.

Interestingly, a cross-correlation peak in the region of 17.2 ppm (^1H) and 166.2 ppm (^{13}C) was also found (Figure 5, dashed squared area). The chemical shift in the proton dimension is more deshielded than that typically found for bicarbonate in ACC (12.4 ppm), indicating that the proton of bicarbonate must be very close to an electronegative species. A similar proton chemical shift for bicarbonate has been observed in the disordered mineral trona ($\text{Na}_3(\text{CO}_3)(\text{HCO}_3)(\text{H}_2\text{O})_2$) at 18.6 ppm.^[33] Based on calculations for an ordered model of trona, a shift of 19.4 ppm is obtained for a species where the proton is almost equally shared between two carbonate ions with distances of 1.18 and 1.25 Å (Table S9). Thus, the proton chemical shift at 17.2 ppm can be tentatively assigned to a $\text{H}(\text{CO}_3)_2^{3-}$ species where the proton is dynamically disordered between two carbonate ions at a short distance.

For ACCs prepared at pH 8.5 and 8.0, identical correlation peaks were found (Figures S19 and S20). In HETCOR spectra, the merging of the carbonate and bicarbonate components correlates well with the increase in the proton chemical shift, suggesting that the acidic protons of some bicarbonate ions are hydrogen-bonded to the neighboring carbonate ions (Figure 5, S19, S21). This intimate interaction between carbonate and bicarbonate may be the clue for

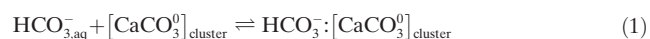
bicarbonate incorporation in ACC, as soon as calcium bicarbonate pre-nucleation association starts to become significant. The fact that bicarbonate constitutes a structural component of ACC shows that it is not simply co-precipitated during the quench. Moreover, the data shows that bicarbonate is only incorporated in the intermediate ACC at pH values where calcium bicarbonate association in the pre-nucleation regime is significant. This unambiguously rules out that random processes based on, for example, charge balancing or surface entrapment play a major role, because bicarbonate incorporation does occur at and below pH 8.5 (97.9% bicarbonate in the buffer, Table S1) but becomes insignificant already at pH 8.8–9.0 (96.8–95.3% bicarbonate in the buffer), that is, at more or less similar total excess amounts of bicarbonate. This strongly suggests that bicarbonate becomes a structural part of ACC due to its binding to the solution PNCs and liquid–liquid-separated calcium carbonate precursors, a possibility which will be quantitatively explored below.

Notably, the thermal stabilities of ACCs prepared at pH 7.5 and 8.0, corresponding to 350 and 359 °C, respectively (Figure S22, Table S11), are greater than the ACCs synthesized by direct mixing of precursor solutions.^[34,35] The enhanced thermal stability can arise due to the surface localization of bicarbonate ions on the nanoscopic ACC constituents within the bulk structure (Figure S22, S23) and also their accompanying hydration molecules, which could prevent their transformation into a crystalline phase, similar to the stabilization of the liquid precursors in aqueous solution. In addition, in post-nucleation sediments collected at lower pH, abundant amorphous nanoscopic particles accompanying vaterite microcrystals are observed (Figure S24–S26). Collectively, these findings indicate the mechanistic roles of bicarbonate ions in stabilizing the liquid precursors and amorphous mineral precursors.

Conclusion

At near-neutral pH, the existence of competition for interaction with calcium ions between carbonate and bicarbonate species produces distinct ion association behavior in the form of PNCs and ion pairs, respectively, the latter of which are negligible only above ca. pH 8.5–9.0. Below pH 8.5, the structural integration of bicarbonate ions can be explained based on the binding of bicarbonate to terminal binding sites of carbonate PNCs and subsequently, upon liquid–liquid demixing, to the interfaces of the nascent nanodroplets. This binding situation has been established in previous simulation work,^[26] and is used as a model here. The observation that the bicarbonate content in solid ACC is constant at around 5%, independent of pH in the near-neutral regime, may reflect the more or less constant bicarbonate fraction in this pH regime (SI Table S1). Indeed, we can formulate the corresponding equilibrium for the binding of bicarbonate to carbonate PNCs and emerging nanodroplets. Assuming that the size distribution of carbonate PNCs does not differ significantly with pH, their concentration is proportional to the constituent ion pairs. Thus, the equilibrium [Eq. (1)], where $\text{HCO}_3^- : [\text{CaCO}_3]_{\text{cluster}}$ represents

bicarbonate ions bound to the terminal binding sites of PNCs, is defined by the equilibrium constant [Eq. (2)].



$$K_3 = \frac{c(\text{HCO}_3^- : [\text{CaCO}_3]_{\text{cluster}})}{c(\text{HCO}_3^-) c([\text{CaCO}_3]_{\text{cluster}})} = \frac{0.05 \cdot c([\text{CaCO}_3]_{\text{cluster}})}{c(\text{HCO}_3^-) c([\text{CaCO}_3]_{\text{cluster}})} = \frac{0.05}{c(\text{HCO}_3^-)} \quad (2)$$

Since the free bicarbonate concentration is of the order of 10 mM and 20 mM, K_3 values are of the order of 5 M^{-1} and 3 M^{-1} at pH 8.5 and lower pH, all respectively. The corresponding standard Gibbs free energies are therefore approximately -4 to -3 kJ mol^{-1} , again, respectively. These values are in excellent agreement with that obtained from computer simulations for the binding of bicarbonate to a calcium carbonate ion pair as a simple model for terminal binding sites of PNCs (SI Table S6). This consideration suggests that the constant fraction of bicarbonate in solid ACC intermediates below ca. pH 8.5 can be quantitatively attributed to a pre-nucleation interaction between calcium carbonate PNCs and bicarbonate ions. In contrast, this observation cannot be well explained based on random processes like bicarbonate surface entrapment, as the total excess of bicarbonate remains large even above pH 8.5 (Table S1), where no significant structural incorporation of bicarbonate in ACC is observed (note that the investigated ACCs were quenched from equilibrated supersaturated—liquid–liquid-separated^[20]—states and not nucleated from solution, ruling out any kinetic effects of different supersaturation levels due to pH differences on their bicarbonate contents). Thus, bicarbonate incorporation appears to rely on the very low fraction of carbonate below pH 8.5, leading to significant bicarbonate binding to stable calcium carbonate PNCs only under these conditions, due to the properties of the law of mass action. Bicarbonate ions have two major influences on the pathways of mineral nucleation; as a soluble species interacting with ionic components, as well as being a structural constituent of the emergent liquid and solid amorphous phases. Indeed, Bewernitz et al.^[28] reported that due to charge effects, bicarbonate incorporation kinetically stabilizes liquid–liquid-separated states on the pathways to crystals, via ACC.

In all, our study reveals the mechanistic contributions of HCO_3^- species towards ion-association during the nucleation of mineral particles and also the progressions and impact of these ionic interactions after particle nucleation, hence identifying novel aspects of physiologically relevant material genesis. These results are crucial for a better understanding of the ionic players in regulating biological and geological mineralization reactions, as well as potentially inspiring synthetic strategies for controlling the growth and structure of minerals. For instance, bicarbonate ions may distinctly alter the interactions of calcium carbonate species with bio-(macro)molecules, especially during the early stages of mineralization, occurring mostly at terminal sites of PNCs and at interfaces of emerging nanodroplets and nanoscopic ACCs. Such a potentially crucial role of bicarbonate has not

been considered in biomineralization mechanisms until now, and bicarbonate may thus indeed be important for controlling mineralization processes in vivo.

Acknowledgements

DG was a Research Fellow of the Zukunftskolleg of the University of Konstanz and partly supported by SFB 1214 (German Research Foundation, DFG) during this work. YCH was supported by a fellowship of the Ministry of Education (Taiwan) during this research. The solid-state NMR measurements were carried out at the Instrumentation Center of National Taiwan University, supported by the Ministry of Science and Technology (MOST-108-2731-M-002-001). PR and JDG thank the Australian Research Council for funding under the Discovery Program (FT130100463 and FL180100087) as well as the Australian Government and Government of Western Australia for providing computational resources through the Pawsey Supercomputing Centre and National Computational Infrastructure. The SEM measurements were performed at the Nanostructure Laboratory of the University of Konstanz. Open access funding enabled and organized by Projekt DEAL.

Conflict of Interest

The authors declare no conflict of interest.

Keywords: amorphous materials · bicarbonate · calcium carbonate · mineral nucleation · NMR spectroscopy

- [1] *Calcium Carbonate: From the Cretaceous Period into the 21st Century* (Ed.: F. W. Tegethoff), Birkhäuser, Basel, **2001**.
- [2] P. G. Vekilov, *Nanoscale* **2010**, *2*, 2346–2357.
- [3] D. Gebauer, P. Raiteri, J. D. Gale, H. Cölfen, *Am. J. Sci.* **2018**, *318*, 969–988.
- [4] D. Gebauer, A. Völkel, H. Cölfen, *Science* **2008**, *322*, 1819–1822.
- [5] L. B. Gower, D. J. Odom, *J. Cryst. Growth* **2000**, *210*, 719–734.
- [6] M. J. Olszta, D. J. Odom, E. P. Douglas, L. B. Gower, *Connect. Tissue Res.* **2003**, *44*, 326–334.
- [7] M. Faatz, F. Gröhn, G. Wegner, *Adv. Mater.* **2004**, *16*, 996–1000.
- [8] Y. Politi, T. Arad, E. Klein, S. Weiner, L. Addadi, *Science* **2004**, *306*, 1161–1164.
- [9] J. J. De Yoreo, P. U. P. A. Gilbert, N. A. J. M. Sommerdijk, R. L. Penn, S. Whitelam, D. Joester, H. Zhang, J. D. Rimer, A. Navrotsky, J. F. Banfield, A. F. Wallace, F. M. Michel, F. C. Meldrum, H. Cölfen, P. M. Dove, *Science* **2015**, *349*, aaa6760.
- [10] L. B. Gower, *Chem. Rev.* **2008**, *108*, 4551–4627.
- [11] Y. U. T. Gong, C. E. Killian, I. C. Olson, N. P. Appathurai, A. L. Amasino, M. C. Martin, L. J. Holt, F. H. Wilt, P. U. P. A. Gilbert, *Proc. Natl. Acad. Sci. USA* **2012**, *109*, 6088–6093.
- [12] T. Mass, A. J. Giuffrè, C.-Y. Sun, C. A. Stiffler, M. J. Frazier, M. Neder, N. Tamura, C. V. Stan, M. A. Marcus, P. U. P. A. Gilbert, *Proc. Natl. Acad. Sci. USA* **2017**, *114*, E7670–E7678.
- [13] R. T. DeVol, C.-Y. Sun, M. A. Marcus, S. N. Coppersmith, S. C. B. Myneni, P. U. P. A. Gilbert, *J. Am. Chem. Soc.* **2015**, *137*, 13325–13333.
- [14] M. H. Nielsen, S. Aloni, J. J. D. Yoreo, *Science* **2014**, *345*, 1158–1162.
- [15] Q. Hu, M. H. Nielsen, C. L. Freeman, L. M. Hamm, J. Tao, J. R. I. Lee, T. Y. J. Han, U. Becker, J. H. Harding, P. M. Dove, J. J. D. Yoreo, *Faraday Discuss.* **2012**, *159*, 509–523.
- [16] E. M. Pouget, P. H. H. Bomans, J. A. C. M. Goos, P. M. Frederik, G. de With, N. A. J. M. Sommerdijk, *Science* **2009**, *323*, 1455–1458.
- [17] M. Kellermeier, D. Gebauer, E. Melero-García, M. Drechsler, Y. Talmon, L. Kienle, H. Cölfen, J. M. García-Ruiz, W. Kunz, *Adv. Funct. Mater.* **2012**, *22*, 4301–4311.
- [18] K. Henzler, E. O. Fetisov, M. Galib, M. D. Baer, B. A. Legg, C. Borca, J. M. Xto, S. Pin, J. L. Fulton, G. K. Schenter, N. Govind, J. I. Siepmann, C. J. Mundy, T. Huthwelker, J. J. D. Yoreo, *Sci. Adv.* **2018**, *4*, eaao6283.
- [19] P. J. M. Smeets, A. R. Finney, W. J. E. M. Habraken, F. Nudelman, H. Friedrich, J. Laven, J. J. D. Yoreo, P. M. Rodger, N. A. J. M. Sommerdijk, *Proc. Natl. Acad. Sci. USA* **2017**, *114*, E7882–E7890.
- [20] J. T. Avaro, S. L. P. Wolf, K. Hauser, D. Gebauer, *Angew. Chem. Int. Ed.* **2020**, *59*, 6155–6159; *Angew. Chem.* **2020**, *132*, 6212–6217.
- [21] P. Raiteri, A. Schuitemaker, J. D. Gale, *J. Phys. Chem. B* **2020**, *124*, 3568–3582.
- [22] M. Kellermeier, P. Raiteri, J. K. Berg, A. Kempter, J. D. Gale, D. Gebauer, *ChemPhysChem* **2016**, *17*, 3535–3541.
- [23] A. F. Wallace, L. O. Hedges, A. Fernandez-Martinez, P. Raiteri, J. D. Gale, G. A. Waychunas, S. Whitelam, J. F. Banfield, J. J. D. Yoreo, *Science* **2013**, *341*, 885–889.
- [24] F. Sebastiani, S. L. P. Wolf, B. Born, T. Q. Luong, H. Cölfen, D. Gebauer, M. Havenith, *Angew. Chem. Int. Ed.* **2017**, *56*, 490–495; *Angew. Chem.* **2017**, *129*, 504–509.
- [25] P. Fantazzini, S. Mengoli, L. Pasquini, V. Bortolotti, L. Brizi, M. Mariani, M. D. Giosia, S. Fermani, B. Capaccioni, E. Caroselli, F. Prada, F. Zaccanti, O. Levy, Z. Dubinsky, J. A. Kaandorp, P. Konglerd, J. U. Hammel, Y. Dauphin, J.-P. Cuif, J. C. Weaver, K. E. Fabricius, W. Wagermaier, P. Fratzl, G. Falini, S. Goffredo, *Nat. Commun.* **2015**, *6*, 7785.
- [26] R. Demichelis, P. Raiteri, J. D. Gale, D. Quigley, D. Gebauer, *Nat. Commun.* **2011**, *2*, 590.
- [27] S. E. Wolf, J. Leiterer, M. Kappl, F. Emmerling, W. Tremel, *J. Am. Chem. Soc.* **2008**, *130*, 12342–12347.
- [28] M. A. Bewernitz, D. Gebauer, J. Long, H. Cölfen, L. B. Gower, *Faraday Discuss.* **2012**, *159*, 291–312.
- [29] D. Gebauer, M. Kellermeier, J. D. Gale, L. Bergström, H. Cölfen, *Chem. Soc. Rev.* **2014**, *43*, 2348–2371.
- [30] D. Gebauer, P. N. Gunawidjaja, J. Y. P. Ko, Z. Bacsik, B. Aziz, L. Liu, Y. Hu, L. Bergström, C.-W. Tai, T.-K. Sham, M. Edén, N. Hedin, *Angew. Chem. Int. Ed.* **2010**, *49*, 8889–8891; *Angew. Chem.* **2010**, *122*, 9073–9075.
- [31] J. K. Moore, J. A. Surface, A. Brenner, P. Skemer, M. S. Conradi, S. E. Hayes, *Environ. Sci. Technol.* **2015**, *49*, 657–664.
- [32] S.-Y. Yang, H.-H. Chang, C.-J. Lin, S.-J. Huang, J. C. C. Chan, *Chem. Commun.* **2016**, *52*, 11527–11530.
- [33] J. Feng, Y. J. Lee, R. J. Reeder, B. L. Phillips, *Am. Mineral.* **2006**, *91*, 957–960.
- [34] A. V. Radha, T. Z. Forbes, C. E. Killian, P. U. P. A. Gilbert, A. Navrotsky, *Proc. Natl. Acad. Sci. USA* **2010**, *107*, 16438–16443.
- [35] J. Ihli, W. C. Wong, E. H. Noel, Y.-Y. Kim, A. N. Kulak, H. K. Christenson, M. J. Duer, F. C. Meldrum, *Nat. Commun.* **2014**, *5*, 3169.

Manuscript received: March 21, 2021
Accepted manuscript online: May 11, 2021
Version of record online: June 18, 2021